Mechanical Properties of Extruded Al-Li-Mg Alloys with Small Cerium Alloying Addition (*)

D.Buttinelli [†], F.Felli, C.Lupi and F.Marani
Department of Chemical Engineering-Metallurgy University "La Sapienza", Rome (Italy)

Abstract

New experimentally die-cast round billets (diam.: 120 mm and length: 500 mm) of Al- Li(2%)-Mg(1-2%)- Ce(0.6-1%) were examined, before and after hot extrusion, to study the effect of Ce-addition on mechanichal properties, particularly fracture toughness and fatigue resistance of as-aged specimens. The influence of cerium on the grain size control and recrystallization was also examined. Microstructure of the alloys was accurately observed by optical and electron metallography (SEM-EDS).
Ageing tests at various temperatures from 150° to 210°C were carried out and the mechanical properties of the alloys determined in aged samples. The positive effect of the cerium addition on the mechanical behaviour of the new alloys was discussed.

Riassunto

Sono state esaminate delle billette cilindriche pressocolate (diametro 120 mm, lunghezza 500 mm) di nuove leghe sperimentali Al-Li(2%)-Mg(1-2%)-Ce(0.6-1%), prima e dopo estrusione a caldo, per studiare l'effetto dell'aggiunta di Ce sulle caratteristiche meccaniche, in particolare sulla tenacità a frattura e sulla fatica di campioni invecchiati. E' stata inoltre esaminata l'influenza del cerio sul controllo del grano e sulla ricristallizzazione. La microstruttura delle leghe è stata osservata accuratamente sia con microscopia ottica che elettronica (SEM-EDS). Sono state condotte prove di invecchiamento a temperature comprese fra i 150 e i 210 °C e sono state misurate le caratteristiche meccaniche delle leghe su campioni invecchiati. E' stato discusso il benefico effetto dell'aggiunta di cerio sul comportamento meccanico di queste nuove leghe.

Introduction

The high interest of Al-Li-based alloys is fundamentally determined by the very low density, especially of Al-Li-Mg alloys, the high elastic modulus and generally good mechanical properties that can be reached after ageing treatments. All transportation systems are potentially interested in these alloys and in the middle of 80's a commercial production of Al-Li-Cu-Mg-Zr alloys (8090, 2091 etc.) was started in USA and Europe by ALCOA, ALCAN and Pechiney and more recently by Martin-Marietta and Reynolds (Weldalite 049) also [1-4].

Other types, such as Al-Li-Mg based alloys, were particularly studied and commercially produced in CSI from 1971 [5]. However, these alloys are very sensitive to impurities, such as iron, and can suffer grain coarsening during thermal treatments.

In previous works [6,7] the effect of cerium and other R.E.metals, as alloying addition to Al-Li-Mg alloys at concentration from 0.3% to 1%, was examined in laboratory-scale small ingots.

Finer grain size in cast alloys, enhanced mechanical properties of the aged samples and strong limitation of the negative effects of the iron impurity were shown. Particularly, all the iron in alloy was found as eutectic constituent $CeFe_2Al_{10}$. Ce-alloying additions have been already used in Al-Li-Cu-Mg-Zr alloys [8,9], but only at low concentrations (<0.3%) and in order to increase the fatigue resistance of the material.

From the previous results [7] the optimal composition range of the alloys was found as follows: Al-Li(2-2.7%)-Mg(1-2%)-Ce(0.4-0.8%)-Ti(<0.2%). The magnesium content was restricted to 2% to avoid strong decrease of the elastic modulus and overageing effect on PFZ [10]. Titanium was selected as grain refiner, in substitution of the commonly used zirconium, in order to produce a more isotropic microstructure. In the

present work experimental results obtained from the first series of semi-industrial scale die-cast and hot extruded alloys are presented and discussed. Particularly, fracture toughness and crack propagation rates from fatigue tests of these alloys are shown and compared to the commercial Al-Li based alloys.

Experimental

The chemical composition of the new experimental alloys is shown in Table 1. Alloys were melt in a silicon carbide crucible (50 kg) and pressure die-cast in a 50 Tons machine as round billets of 120 mm diam. and 500 mm length. Commercial grade aluminium (0.3% Fe and <0.1% Si), pure magnesium (99.95%), technical grade lithium (98%) and cerium (99%) were used. Titanium was added as aluminium master alloy containing Ti 10% and B 2%. Hydrogen degassing, by argon bubbling immediately before die-casting, was also performed.

Billets were machined to reduce diameter to 110 mm, then controlled for eventual internal defects by X-rays methods, homogenized at 510°C for 20 hours in an inert atmosphere and finally extruded at 490°C with 6.5 reduction ratio.

TABLE1 - Chemical composition of the alloys (Al bal.)

	density (g/cm³)	Li	Mg	element (%) Ce	Fe	Ti
A-alloy	2,50	1,75	0,80	0,65	0,32	0,15
B-alloy	2,48	2,01	1,83	0,98	0,31	0,16

Specimens for mechanical testing were cut from die-cast billets or extruded rod. Ageing tests were carried out in the temperature range from 150° to 210°C after solution treatment (530 °C - 3h). Fracture toughness was measured according to ASTM E-399, fatigue tests (ASTM E-647) were performed in laboratory air at frequency of 10 Hz, sinusoidal load with a ratio R=0.3, on CT specimens of dimensions: B = 10 mm, W = 36 mm. Crack plane orientation code is shown in Fig. 1. The experimental results were processed by a computer program to obtain the da/dN-ΔK curves. Collipriest's semi-empirical relation[11] was used to interpolate the experimental data. Metallography and fracture surface examinations were carried out by light microscope and SEM-EDS.

Result and Discussion

Microstructures of die-cast and extruded alloys are shown in Fig. 2. Grain size appeared almost coarse but a completely isotropic structure was also maintained after extrusion. The constituent of the typical eutectic structure, $CeFe_2Al_{10}$ is shown in Fig. 3.

All the iron was present in such a phase and no acicular $FeAl_3$ was observed, so confirming the primary effect of cerium in alloy as tramp element for the iron-impurity. The excess of cerium concentration, such as in B-alloy caused the presence of other phases, e.g. $CeAl_4$, $CeMgAl_{12}$ and coarse precipitates of TiCe, containing also some aluminium, with average dimension of 15 μm, as shown in Fig. 4. Because of the low

solubility of these phases in aluminium matrix, an incoherent precipitates distribution was generated inside the grains after hot-working and the grain growth was limited.

Typical ageing curves at various temperatures of die-cast or extruded specimens are illustrated in Fig. 5. It is clearly evident that A-alloy with an insufficient Li-content showed a very small increase of hardness at all temperatures. B-alloy hardened quite well at 180°C, but fast over-ageing could be reached in very short time, particularly in extruded specimens. At 150°C the hardening was less critical, but the level of hardness was much lower. Conclusively, the peak-ageing condition was obtained after 20-50 hours at 180°C.

Tensile properties practically confirmed the ageing curves. A-alloy showed, as it is illustrated in Fig. 6, very poor resistential level, achieving a maximum of 140 MPa of UTS after peak-ageing in as-cast condition and 200 MPa in as-extruded and aged samples. However, B-alloy presented very interesting values, particularly as extruded and aged samples, reaching more than 350 MPa of UTS together with an acceptable elongation at rupture of more than 10%, as shown in Fig. 7. From this fact, it can be supposed that increasing the lithium content of alloy up to 2.5-2.8% excellent tensile properties can be easily obtained.

The tentative of enhancing the mechanical properties of B-alloy by the "stretching" effect, was tried, as suggested also by Harris et al. [10], who examined Al-Li(2%)-Mg(2-6%)- Zr(0.2%) alloys. Particularly, they found a notable increase of UTS and 0.2% P.S., approximately by 10%, after a 5% stretching. Moreover, in the alloy Al-2Li-2Mg-Zr, the precipitation phenomena of the phase Al_2MgLi at grain boundary during overageing, with subsequent formation of precipitate free zones (PFZ), was less pronounced and the best combination of tensile properties and fracture toughness was achieved by peak-ageing after stretching. However, in this work, as it can be seen in Table 2, the B-alloy did not show any notable increase of the tensile resistance by stretching before ageing, even if the alloy presented a coarse grain size and the plastically deformed matrix by stretching would have been able to create very large quantity of nucleation sites for δ^1 precipitation and then a more fine and homogeneous distribution of precipitates. Probably, a possible explication could be the high density of pre-precipitated phases, such as $CeFe_2Al_{10}$, $CeAl_4$ and others, which locally caused a highly deformed matrix inside the grains, so vanifying the effect of stretching. The moderate amount of the Li-content in the alloy must be also considered. Effectively the only influence of stretching was a light increase of 0.2% P.S. and again in ductility, as it is shown from the increase of El. % and R.A., by comparing samples peak-aged at 180°C (50 hours) with and without stretching (Table 2).

TABLE 2 - Tensile properties of B-alloy

	0,2% P.S. (MPa)	U.T.S. (MPa)	El. %	R.A. %
S.H.T. at 530 °C	85	229	22,0	33,3
Aged at 180 °C (17 hours)	208	353	11,7	19,6
Aged at 180 °C (50 hours)	222	370	11,3	16,7
Aged at 180 °C (70 hours)	251	363	11,4	19,0
Aged at 200 °C (10 hours)	180	290	12,0	27,7
4% stretched and aged at 180 °C (3,5 hours)	229	322	12,9	17,7
4% stretched and aged at 180 °C (10 hours)	229	320	11,2	17,7
4% stretched and aged at 180 °C (50 hours)	247	326	13,7	28,2

Fracture toughness values (KQ) of B-alloy are shown in Table 3 together with commercial alloys 8090 and

2091. All the fracture toughness values were good, the most critical directions appeared to be C-R (circumferencial - radial) and R-L (radial - longitudinal), in both cases the crack path was growing on the same plane, but along different directions.

TABLE 3 - KQ values of B-alloy compared with 8090 and 2091 alloy

Alloy	Direction	K_{IC}, K_Q (MPa $\sqrt{m}$)
B-alloy	CR	25
B-alloy	RL	25
B-alloy	LR	31
8090 T8XX	TL	23
8090 T8XX	LT	24
8090 T8XX	ST	15
8090 T8XX	SL	14
2091 T8X51	LT	36
2091 T8X51	TL	34
2091 T8X51	SL	24

B-alloy, compared with commercial alloys 8090 and 2091, showed higher fracture toughness values in the most critical directions and equal along the most tough one (L-R). But fracture toughness values of B-alloy are not too different along the different directions, so confirming that B-alloy has an excellent isotropic structure.

The results of fatigue crack growth rate tests of B-alloy along the three different directions are shown in Fig. 8. In this figure the experimental points have been interpolated by the Collipriest model curves with coefficients m=4.46 C= $9.37*10^{-13}$ for R-L and C-R directions and m=3.037 C= $3.52 * 10^{-11}$ for L-R one . It is easy to observe that also in this case the fracture crack growth rate values are distributed in a small range, as a consequence of the isotropic structure of this alloy. Similar tests performed on a commercial 8090 alloy have shown that along the most critical directions, SL and ST of a sheet plate, the fatigue crack growth rates are quite larger than along the other directions (TL and LT) showing the high anisotropy of this alloy [12].

Fig. 9 shows the Collipriest's model curves of B-alloy in comparison with commercial 2091 and 8090 alloys, as it is illustrated in other papers [12, 13]. It is easy to observe that crack growth rates of B-alloy are lower, with larger ΔK_{th}. Only for high ΔK values 2091 alloy shows lower crack growth rates. The morphology of fatigue fracture of B-alloy is correlated to the direction of crack path. Along C-R and R-L directions the fracture surfaces are similar, even if the first runs across the extrusion direction and the second along that direction. The fracture surfaces were quite ductile, as confirmed by the large amount of dimples as shown in Fig. 10, particularly at higher ΔK values they showed pronounced roughness and the fracture was almost completely transgranular. $CeAl_4$ and $CeFe_2Al_{10}$ phases along the crack path did not cause fragilization phenomena, but Ti-Ce phase showed a fragile interface along the crack path as shown in Fig. 11. It is very important to observe that delamination, which is one of the typical phenomena in the Al-Li alloys fracture behaviour, has never appeared in B-alloy. Some fatigue striations are visible on the crack path.

Closing effects were highly pronounced, as shown in Fig. 12, by fretting deposits and production of lithium oxides. Along L-R direction the fracture surface was even more rough and fretting deposits appeared also, the surface was very oxidated and large cleavage planes were present also as illustrated in Fig. 13.

Along this direction $CeAl_4$, $CeFe_2Al_{10}$ and Ti-Ce phases were found only in a few cases on the crack surface, and it seemed that the crack tip by-passed them and failured the matrix around them only.

Conclusion

It has been defined a technology to produce ingots of Al-Li-Mg-Ce alloys on a semi-industrial scale, with good global mechanical properties. During this first step some alloys with different chemical compositions have been produced by using this technology. The mechanical properties reached good levels with lithium content near to 2%, so it is reasonable to forecast large increments increasing the lithium content up to 2.5-3%, as already shown by the alloys produced in small ingots[7]. Fracture toughness values (K_Q) were good, higher than those of commercial Al-Li alloys in some directions, and not too different along the other directions, so confirming that these alloys have an excellent isotropic structure, compared to the commercial ones.

Aknowledgement

References

[I]   R.Grimes et al., in *Aluminium-Lithium* (M.Peters and P.J.Winkle\r, eds.), DGM, Oberursel, 1992, pp.3- 14.
[2]   R.H.Graham, R.J.Rioja and J.M.Newman, ibidem, pp. 15-24.
[3]   D. Constant, M.Doudeau and R.Mace, in *Aluminum-Lithium Alloys* (T.H.Sanders and E.A.Starke, eds.), MCEP, Birmingham, 1989, pp.65-73
[4]   W.T.Tack et al., in *Aluminum-Lithium* (M.Peters and P.J.Winkler, eds.), DGM, Oberursel, 1992, pp.409-414.
[5]   I.N.Fridlyander, A.G.Bratukhin and V.G.Davydov, ibidem, pp. 35-42
[6]   D. Buttinelli, F. Felli, C. Lupi and F. Marani, ibidem, pp.433-438.
[7]   D. Buttinelli, F. Felli, C. Lupi and F. Marani, in *Light Materials for Transportation Systems* (N.J.Kim, ed.), CAAM-PUST, Pohang (Korea), 1993, pp.l41-149.
[8]   Z.Baochang et al., in *Aluminum-Lithium Alloys* (T.H.Sanders and E.A.Starke, eds.), MCEP, Birmingham, 1989, pp. 529-535.
[9]   M. He et al., in *Aluminium-Lithium* (M.Peters and P.J.Winkler, eds.), DGM, Oberursel, pp. 563-568.
[10] S.J.Harris, B.Noble and K.Dinsdale, in *Aluminium-Lithium Alloy* II (T.H.Sanders and E.A.Starke, eds.), TMS-AIME, 1983, pp. 219-234.
[11] J.E. Collipriest, *An experimentalist's view of the surface flaw problem* ASME, 1972 pp.43-72.
[12] M.Cavallini, F. Felli, P.Delogu, *Composite fracture in AlLiCu Alloy*, Metallurgical Science and Technology, 1991, vol.9 no.1 pp. 3-9.
[13] M.Cavallini, F. Iacoviello, F. Felli, in *IX Convegno Nazionale del Gruppo Italiano Frattura*, 1993, pp. 171-179.
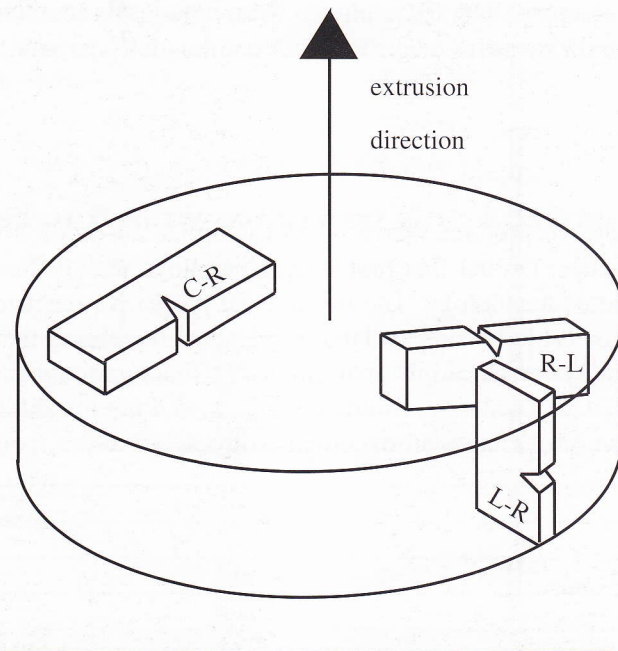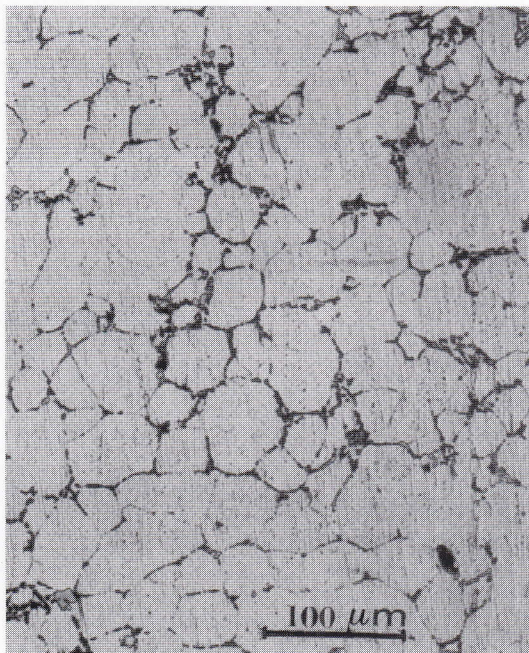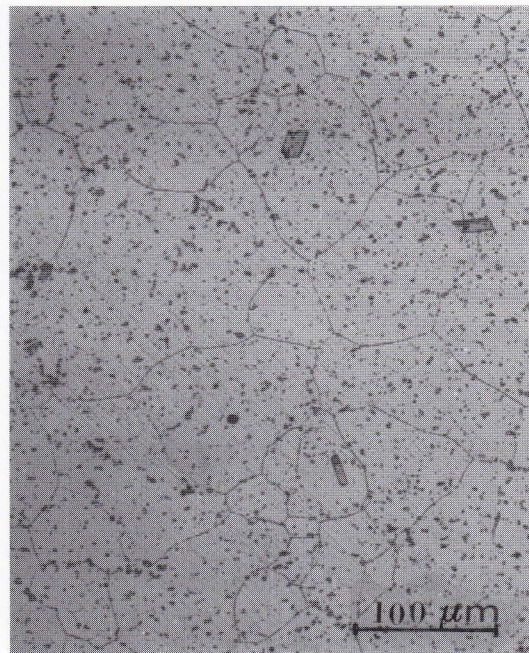
Fig. 1:
Crack plane orientation code for bar

(A)   (B)

Fig. 2:
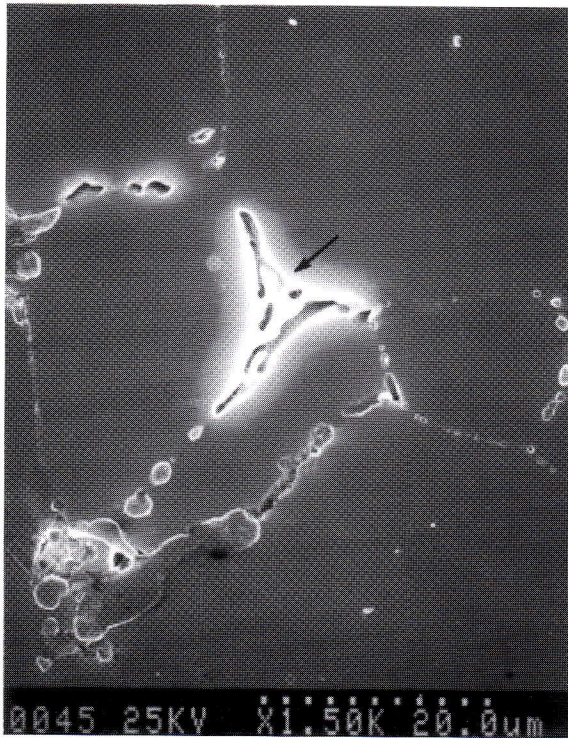(A) Microstructure of as-die-cast and (B) as-extruded B-alloy

Fig. 3:
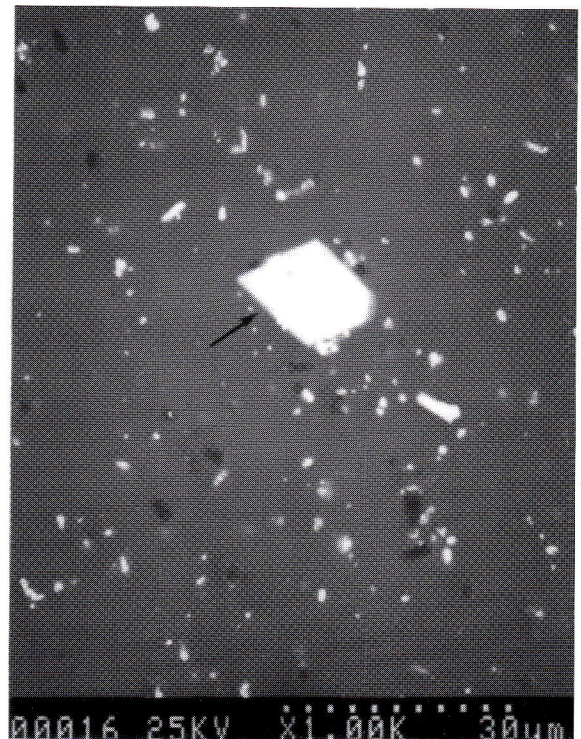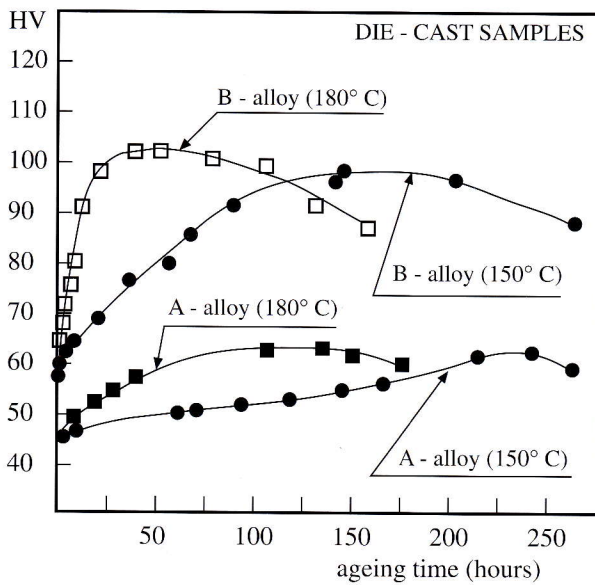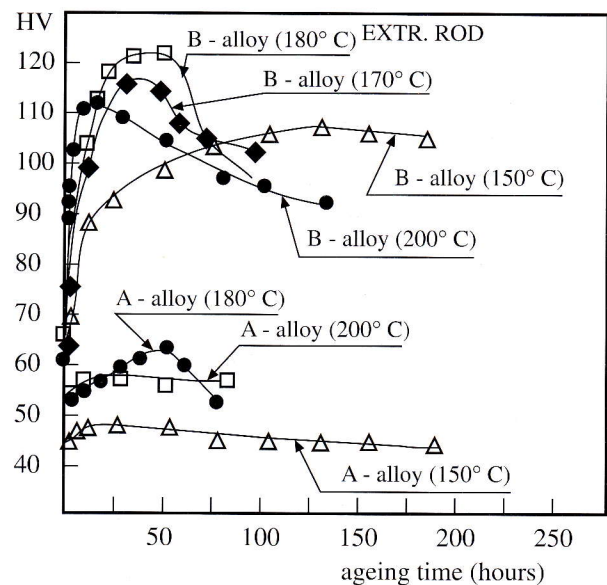Micrograph of $CeFe_2Al_{10}$, constituent of the typical eutectic

Fig. 4:
Microstructure of B-alloy with coarse precipitate of TiCe

(A)

(B)

Fig. 5
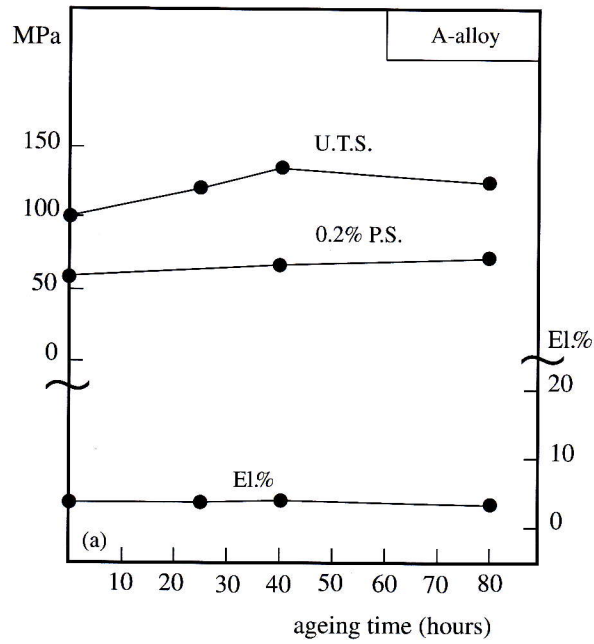Ageing curves of (A) die-cast and (B) extruded specimens

Fig. 6:
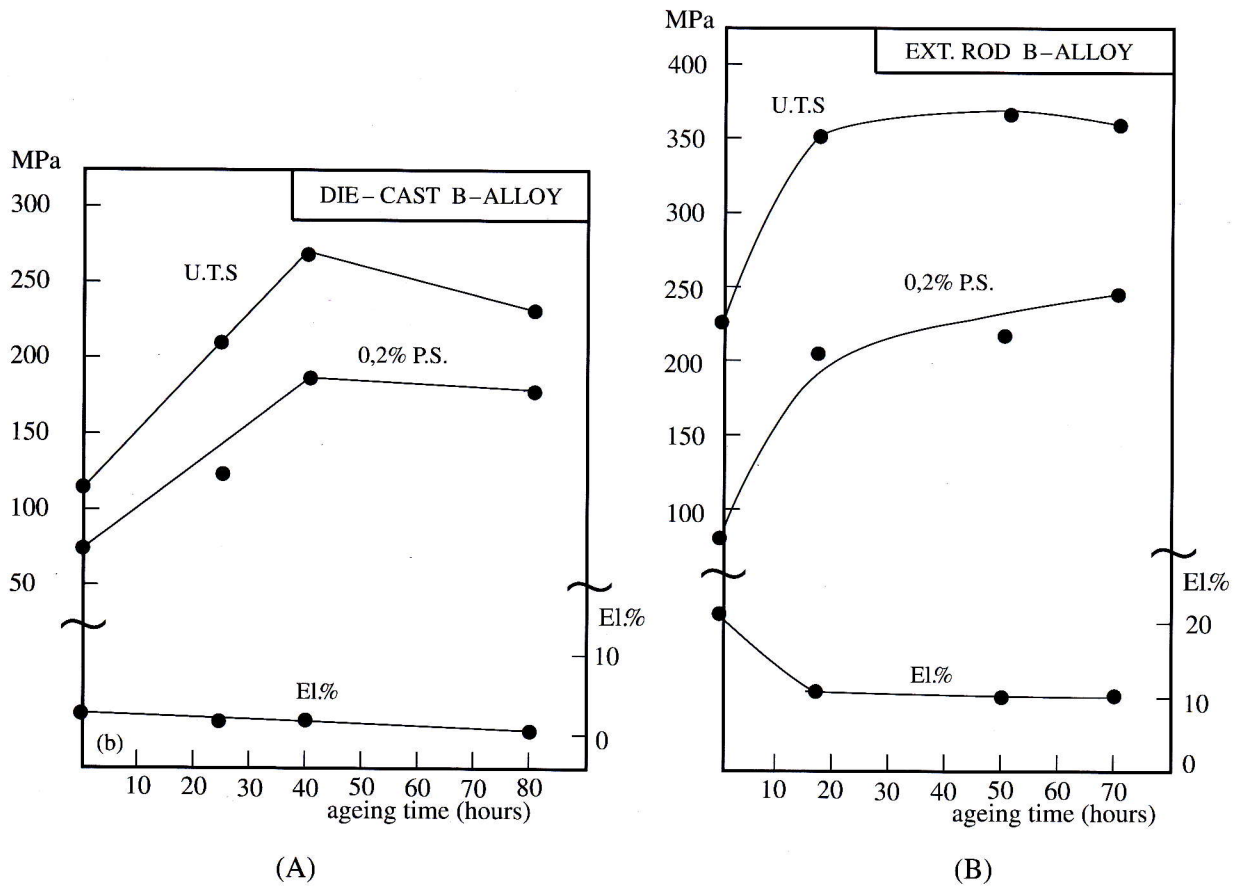Tensile properties of as-die cast A-alloy vs. ageing time (180 °C)

(A)   (B)

Fig. 7:
Tensile properties (A) of as-die-cast and (B) of as-extruded B-alloy vs. ageing time (180 °C)
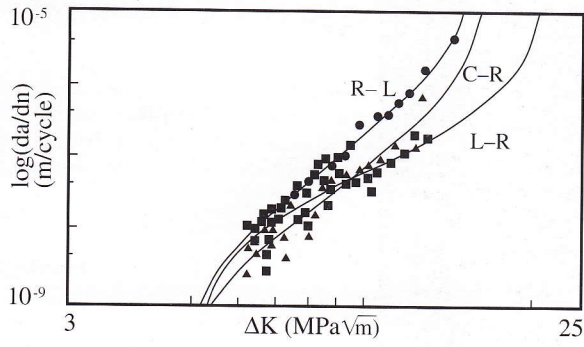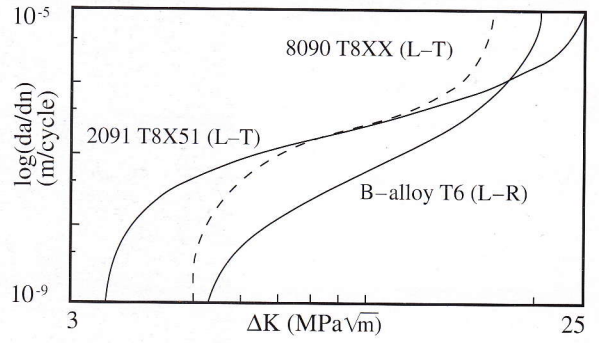
Fig. 8
Fatigue crack propagation tests on B-alloy

Fig. 9
Comparison between Collipriest's models
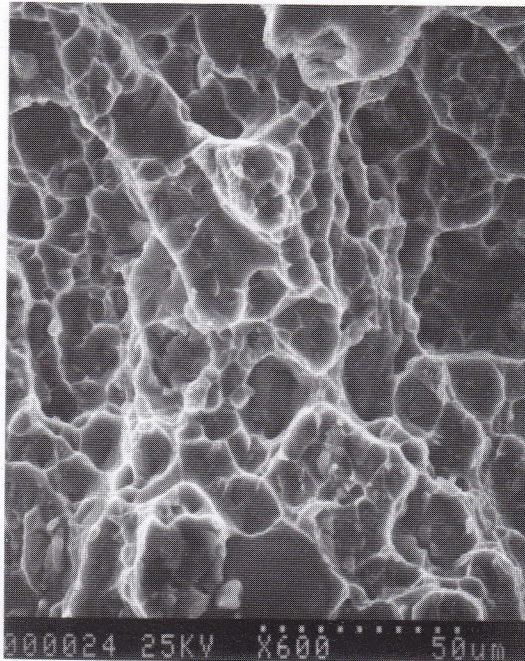of B-alloy and commercial alloys

Fig. 10:
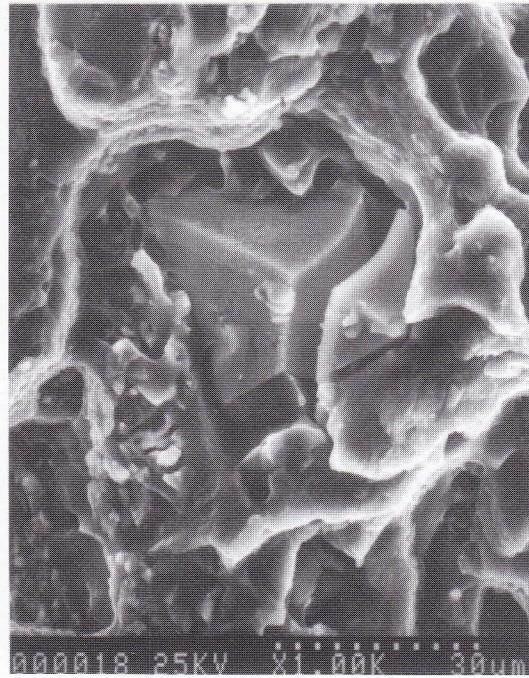Dimples on fracture surface of B-alloy

Fig. 11:
Ti-Ce fragile interface along the crack path
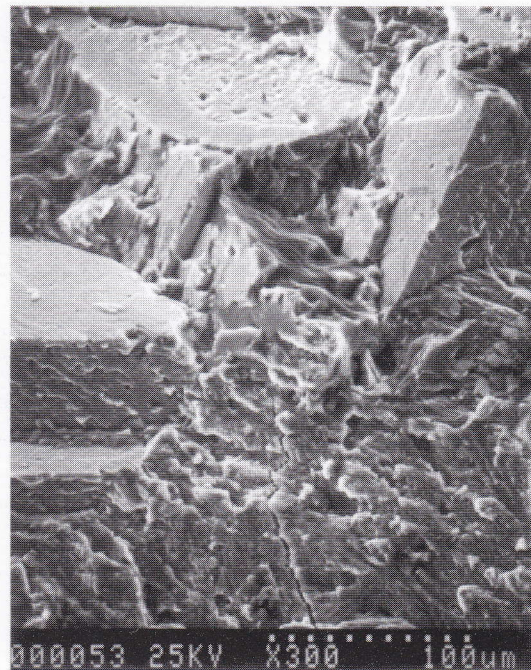in B-alloy

Fig. 12:
Fretting deposits on crack surface of B-alloy

Fig. 13:
Cleavage planes on crack surface of B-alloy